

# Microstructural and Corrosion Behaviour of Discrete Arced Weld Droplets Deposited on Sugarcane Roller Shells

V.E. Buchanan<sup>1</sup>, PhD

<sup>1</sup>University of Technology, Jamaica, vbuchanan@utech.edu.jm

**Abstract**– This article reports on the relationship between the arcing current and the microstructural and corrosion behaviour of discrete weld droplet deposited on sugar mill roller shells made from grey cast iron during hardfacing in a typical sugarcane factory.

Hardfaced droplet deposits were removed from three simulated roller shells, which were arced with different current, and subjected to porosity, microhardness and corrosion tests. The results revealed that the percentage porosity, microhardness value and corrosion rate significantly depended on the welding current; the rate of corrosion generally increased with a decrease in porosity and an increase in microhardness.

**Keywords**--: sugarcane, weld droplet, hardfacing, roller shell, corrosion.

## I. INTRODUCTION

Sugar is manufactured from the sugarcane plant (*Saccharum Officinarum*), which is harvested and taken to the factory where it undergoes a number of processes. A train of three-roller mills are used to crush the sugarcane and extract the sucrose-rich juice, and grey cast iron is the commonly used material for making the roller. Prior to milling, the surface of the roller, which is machined with a series of V-shaped grooves around the periphery and evenly spaced along its length, is roughened by a process called “roller arcing” in which discrete weld droplets are deposited onto the crests and flanks of the roller teeth [1]. The arcing is generally carried out in-situ while the roller is rotating at high speed so that the weld is made intermittently around the roller. The rough surface enhances the natural gripping action of the roller and ensures consistent feeding of the bagasse through the mill, as well as to prolong the life of the roller [2]. The bagasse is the residue left after the extraction of the cane juice.

Although the arcing of rollers has been in usage for over 60 years [3, 4], the process has greatly improved with the development of automated roll arcing machine [2, 5]. Fe-Cr-C based alloys are most commonly used to arc the rollers; the presence of chromium provides corrosion resistance and the hard chromium carbide precipitates increase resistance to abrasion.

Roller arcing appears to meet the needs in terms of reduction in slippage of the bagasse on the roller teeth and improvement in extraction [6]. The moisture content in the bagasse produced at the end of the crushing process was seen to increase as the surface of the roller shells lost its roughness, thus indicating the decreased effectiveness of the roughened surface. This is used as a parameter for indicating the effectiveness of arcing sugar mill rollers. However, the weld

droplets are used in a corrosive environment as the sugarcane juice is acidic with pH value at around 4.5 [7] due to microorganisms in sugar juice, and this reduces their gripping ability and wear resistance. Additionally, unwanted cracks and porosity formed within the weld and heat-affected zone can trap the cane-juice and cause severe corrosion problem, resulting in the premature failure of the welds, and lead to the expose of the substrate and accelerated wear rate [1]. Nevertheless, Oliver [7] reported that it is not a conclusive parameter as it is dependent on additional factors such as the degree to which the sugarcane has been prepared, the percentage imbibition (spraying of water on the crushed cane fibre as it emerges from each milling unit, except the last one, to increase the extraction of cane juice) and the morphology and anatomy of the sugarcane. Additionally, the process is very inefficient and labour-intensive, many of the weld deposits are broken off in service, and cracks are produced within the iron phosphide eutectic regions in the heat-affected zone of the weld [8]. The cost associated with this method can be high as the process may involve disassembly, re-grooving and re-installation of the rollers.

While studies have been done on hardfacings, little study has been undertaken on the individual weld droplets in the as-deposited condition. Therefore, further study needs to be conducted to determine the overall benefit of roller arcing, particularly as it relates to dilution and corrosion of the weld droplets. Hence, the aim of this study is to examine the microstructural and corrosion behaviour of the arced droplets in the presence of sugarcane juice.

## 2. EXPERIMENTAL DETAILS

### A. Materials

Grey cast iron discs were machined on the lathe to the size and shape shown in Fig. 1, which represents the typical tooth profile of a mill roller. The chemical composition of this alloy is given in Table 1.

Roller arcing on the tapered face of the disc was carried out using the Elarc Mill Arc 80 shielded metal arc welding electrode, which is specifically designed to deposit discrete hardfacing welds on rotating mill rollers made of grey cast iron. The chemical composition of the electrode is given in Table 1. The dry arcing process was carried out while the disc rotated at a surface speed of 245 mm/s, which is typical to that of a sugarcane mill roller. Arcing was achieved by setting up an arcing rig on a centre lathe in conjunction with a slip ring and brush assembly (Fig. 2) that prevented damage to the headstock bearings of the lathe. Arcing was carried out with a Hobart constant current rectifier TR-250 welding equipment, using direct current electrode positive, which imparts deeper weld penetration. Three discs were arced, each at a current of 115,

Digital Object Identifier (DOI):

<http://dx.doi.org/10.18687/LACCEI2019.1.1.360>

ISBN: 978-0-9993443-6-1 ISSN: 2414-6390

130, and 140 A, respectively. These values spanned the range (115 – 140 A) recommended by the electrode manufacturer. After the discs were arced, they were allowed to cool under ambient condition to room temperature. Subsequently, a minimum of 15 discrete weld droplets of approximately 2 to 3 mm diameter were randomly removed from each disc for testing.

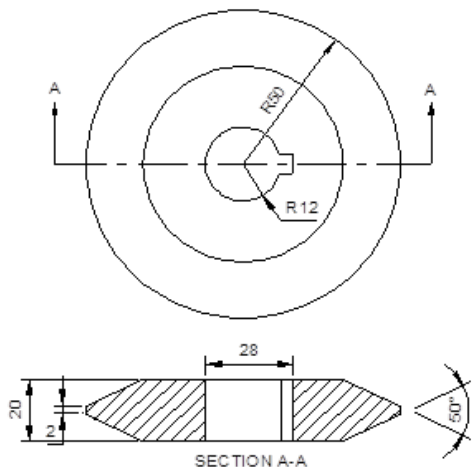


Fig. 1 Preparation of grey cast iron disc for arcing. Dimensions are in millimeters

### B. Microstructural Characterisation

Porosity (which appeared dark in the polished surface) of the weld droplets was analyzed using the Zeiss Axiotech optical microscope in conjunction with an image analyzer software, using an MC 80DX video camera attachment. Each field was approximately  $227 \times 171 \mu\text{m}$ , and measurements were carried out on 25 randomly selected locations for each specimen. The percentage porosity was then determined by the point counting method, i.e.,

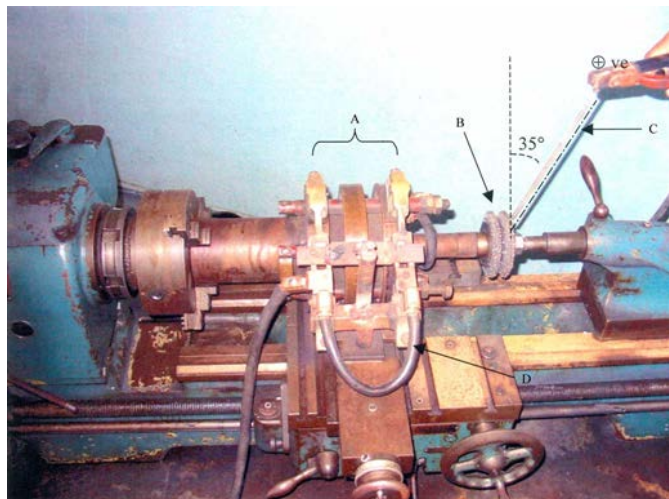
$$\% \text{Porosity} = \frac{\text{No. of pores}}{\text{No. of grid points}(30 \times 30)} \times 100$$

TABLE 1

Chemical composition (wt. %) of grey cast iron disc and welding electrode

Element	Cast Iron	Electrode	
		Wire	Coating
C	3.45	-	8.74
Cr	0.14	0.06	41.8
Mn	0.38	0.30	1.9
Si	2.41	0.02	3.9
P	0.09	<0.005	<0.005
Ni	0.08	0.07	0.11
Cu	0.22	0.20	-
Mo	0.03	0.006	0.007
S	0.08	0.049	<0.005
Fe	Bal	Bal	-
Al	-	-	0.52
Ca	-	-	1.1
Mg	-	-	0.24
Ti	-	-	0.67
V	-	-	0.053

The weld droplets were radially cut into two parts using a sectioning machine. The cut-off disc used was aluminium oxide with a thickness of 0.38 mm and diameter of 100 mm, supplied by Allied HighTech, USA. Cutting was operated at 0.01 mm/s feed rate and 2500 rpm wheel speed. Five weld droplets from each disc were then mounted together in phenolic resin with the cut sections exposed in order to facilitate analysis from the outer to the inner section of the weld droplet. For each type of test conducted (corrosion, microhardness test, and microstructural examination) three sets of mounted specimens were made, each representing an arced disc of specific amperage.



A – Slip ring and brush assembly; B – Mill roller disc specimen with droplets being deposited; C – Welding electrode; D – Negative cable lead from welding machine

Fig. 2 Setup of arcing rig assembled on a lathe to deposit weld droplets on disc

For optical examination, the specimens were polished using a 0.3- $\mu\text{m}$  and 0.05- $\mu\text{m}$  alumina paste for coarse and final polishing, respectively, washed with soap and water, and then rinsed in alcohol and dried by blowing warm air over each specimen. The polished specimens were etched with an Acid-Ferric Chloride (5.0 g  $\text{FeCl}_3$  + 50 ml  $\text{HCl}$  + 100 ml  $\text{H}_2\text{O}$ ) solution. A LEO 1530 scanning electron microscope (SEM) with an EDX attachment and operating with an accelerating voltage of 15 kW was also used to further examine the microstructure at higher magnification and to determine the elemental analysis, using line scan, of the droplets.

Microhardness measurements were conducted with a HM-123 Mitutoyo digital video Vickers microhardness tester, using a load of 0.5 kgf for 15 seconds. All hardness measurements were taken on unetched specimens with surfaces ground to 800-grit paper and polished with a 1- $\mu\text{m}$  silicon carbide paste. At least five indentations were made on each specimen.

### C. Corrosion Testing

For corrosion testing, each specimen was ground with a series of silicon carbide emery paper from 120 to 600 grades,

after which the specimens were washed with distilled water, then with acetone, and dried using a stream of warm air. The specimens were weighed on an OHAUS electronic scale having a resolution of 0.0001g, and then suspended in a 500-ml beaker containing 350 g of artificial sugarcane juice that was made by mixing 50 g of molasse with 300 g of distilled water. The pH of the solution was 5.5. Each beaker contained five weld droplets from each of the three discs, and all tests were conducted at the same time. The immersion test was conducted at a temperature of 25 °C for a period of 50 hours and was open to the atmosphere. Following the tests, the specimens were washed and brushed to remove any residue or scales, and then dried in an oven heated to 100 °C for 40 minutes to remove any moisture that might have penetrated into the pores. They were then reweighed in order to determine the average weight loss due to the effect of corrosion. The corrosion rate, in mm/year, was calculated using the expression:

$$\text{Corrosion Rate} = \frac{87600 \times \text{Weight Loss}(g)}{\text{Density}(g/cm^3) \times \text{Area}(cm^2) \times \text{Time}(hr)} \quad (2)$$

## 2. RESULTS AND DISCUSSION

### A. Microstructure

Figs. 3 and 4 show typical optical micrographs of the microstructure of the weld droplets, arced at 115 and 130 A, respectively. Generally, there were variations in the microstructure from one weld droplet to the next, even when deposited under the same conditions. The reason for this variation is attributed to the ad-hoc alloying burn-off of the electrode [9]. Despite the variations, the representative microstructure is a network of primary  $M_7C_3$  carbide (the lighter section) in a eutectic matrix of austenite (the dark region) and smaller  $M_7C_3$  carbides, which was previously confirmed on the basis of the x-ray diffraction phase identification, energy dispersive spectroscopy analysis and microhardness values [10]. Both needle and platelet type morphologies of the  $M_7C_3$  carbides are observed in the plane of polish with their long axes parallel to the heat flow direction of the weld. These carbide morphologies have also been described by other researchers [11, 12].

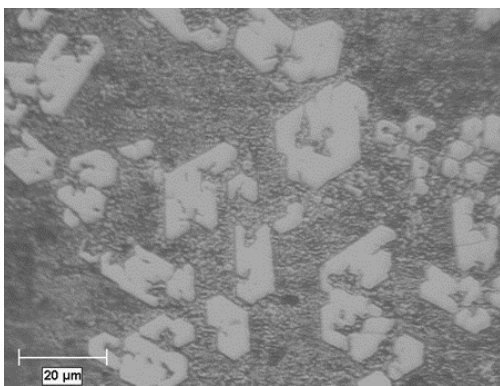


Fig. 3 Typical optical micrograph of the radial section of the arced weld droplets at 115 A

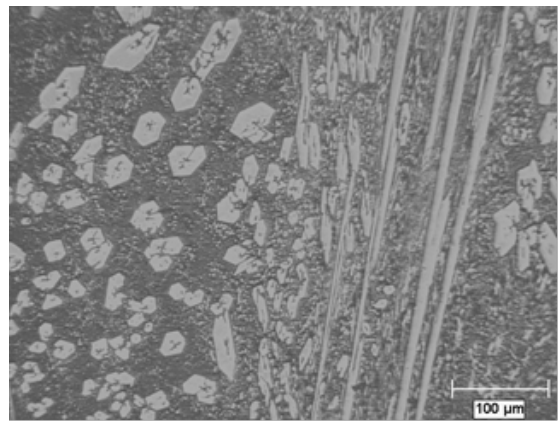


Fig. 4 Typical optical micrograph of the radial section of the arced weld droplets at 130 A

Table 2 shows the average elemental analysis of the weld droplets in the fusion zone and in the sheared zone (the region that was sheared from the parent metal). Considering the amount of chromium in the electrode coating, it appears that the expected benefit of the first layer of droplet is not realized, unless additional layers are added. It is also obvious that there is a wide disparity in the amount of chromium and carbon in the weld droplets, causing the weld droplets to have a higher probability of being locally attacked because of microsegregation in the structure. Pits, for example, can form as a result of the concentration cell established by the compositional variation in the droplet giving rise to localized anodic and cathodic regions, which will ultimately affect the behaviour of the individual droplet during the crushing of the sugarcane, thus contributing to the concerns mentioned earlier by French [9].

TABLE 2  
Average elemental analysis (wt.%) of the weld droplets. The ‘±’ represents one standard deviation of the mean.

Location	C	Cr	Mn	Fe	Si
Fusion zone	6.58	20.91	2.10	67.99	2.42
	± 2.57	± 2.86	± 0.92	± 3.81	± 1.42
Sheared zone	7.04	2.63	0.29	86.64	3.40
	± 2.99	± 0.83	± 0.35	± 2.98	± 0.55

### B. Porosity

Porosity is one of the most common weld defects and is caused by entrapped gases, usually hydrogen) which originates from oil/grease or from moisture in or near the weld zone during welding. Fig. 5 shows a typical SEM image of the fractured surface of a droplet that was removed from the disc. It is obvious that several pores are visible on the surface. The average amount of porosity was determined by the conventional point counting technique, and the results are presented in Table 3. According to the results, there is a polynomial relationship between the welding current and porosity with the minimum porosity of 6.6% obtained with an arc current of 130 A specimens exhibiting the least porosity.

Arc current, voltage and polarity have the biggest effects on porosity; increasing the arc current and voltage reduce

porosity while DCEP increases porosity [13]. Although higher heat input increases solidification time thereby allowing more time for gas to escape from the weld pool, the high porosity at 140 A could be attributed to shrinkage void as a result of the higher solidification gradient as well as the increase turbulent flow of the weld pool.

Porosity creates poor coating cohesion and allows for higher wear as it provides easy fracture paths for crack propagation and the eventual loss of material. Porosity is also associated with a higher number of unmelted or partially-melted particles which become trapped in the coating [14].

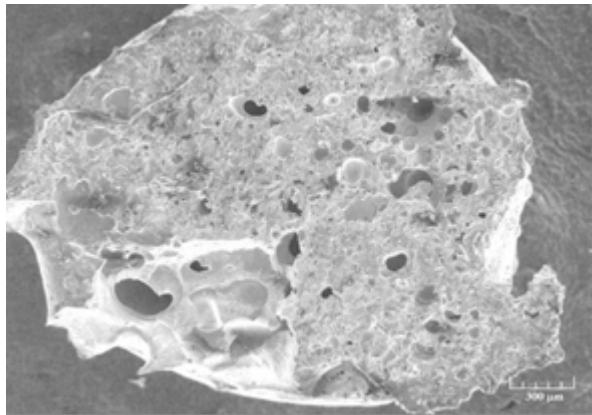


Fig. 5 SEM image of the fractured surface of a weld droplet (130 A) sheared off the disc

TABLE 3

Quantitative analysis of weld droplets arced at different current. The ‘±’ represents one standard deviation of the mean.

Welding Current (A)	Average Porosity (Vol.%)	Microhardness (HV)	Corrosion rate (mm/yr)
115	22.4 ± 4.8	634 ± 53	1.79
130	6.6 ± 2.6	795 ± 100	1.16
140	21.0 ± 5.7	729 ± 72	1.57

### C. Microhardness

Table 3 shows the average microhardness values of the droplet deposits. The hardness of the weld droplets is clearly greater than the base metal (198 HV), the large scatter resulting from the difference in hardness of the microstructural constituents and the compositional variation. The hardness varied with welding current with the 130-A weld droplets exhibiting the highest hardness value. Although the hardness at 130 A is not statistically different to the 140-A, there was a significant difference ( $p = 0.01$ ) when compared with the 115-A weld droplets. These results confirm a previous study [7] which showed no direct relationship between current and hardness. Rather, the microhardness values indicate that there is a polynomial relationship between current and microhardness within the range tested in this study.

There is also a strong correlation of microhardness with porosity ( $r = 0.85$ ), which suggests that porosity has a major

influence on hardness. Since care was taken not to measure the hardness in areas in close proximity to a pore, the variations in hardness and the higher hardness at the midrange current may be explained in terms of the microstructure. It is known that higher amperage increases dilution of the weld [15]; thus, hardness decreases. Furthermore, lower amperage results in less precipitation of the chromium rich particles from the electrode with a consequent change in microstructure from the expected hypereutectic to either eutectic or hypoeutectic.

### D. Corrosion

Gravimetric study was conducted on the specimens to determine corrosion characteristics. Table 3 shows that corrosion rate decreases as the arcing current increases from 115 to 130 A, where the measured value was 1.16 mm/year. However, at the highest current (140 A), the corrosion increases to 1.57 A, and this may be attributed to the higher percentage porosity at the same current. Therefore, corrosion is strongly influenced by the microstructure.

Fig. 6 shows an optical micrograph of the droplet (at 130 A) immersed for 50 hours in the prepared cane juice at 29 °C. Visual examination of the corroded surfaces of the weld droplets showed the presence of corrosion products covering most of the surface, particularly the austenite matrix. The uncorroded region (the lighter area) is the  $M_7C_3$  carbides. The microstructure consists of an anodic region (austenite/ferrite) and a cathodic region ( $M_7C_3$  carbides), and with the cane juice acting as an electrolyte, a galvanic cell develops between the anodic and cathodic region, leading to the dissolution of iron.

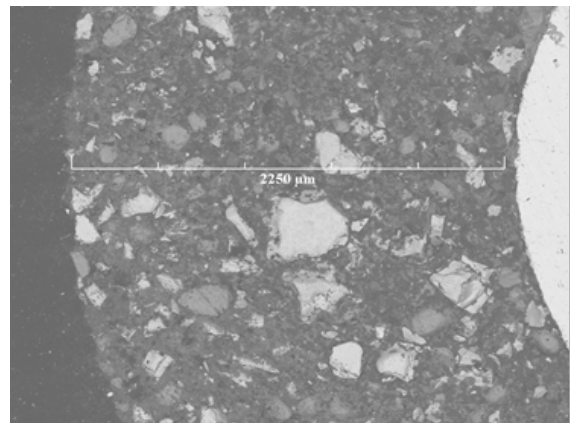


Fig. 6 Optical micrograph of weld droplet immersed for 50 hours in cane juice (sucrose) at 29 °C

Following the removal of the corrosion products from the surface by hard brushing, pits were clearly visible. Since the weld droplets consist of minor alloying elements and impurities, Davis [16] argues that different electrochemical characteristics will be present which leads to accelerated corrosion in localized regions properties. Since the carbide phases are cathodic to the austenite/ferrite phases (the anode),

the carbides will project above the austenite/ferrite phases, exposing the leading edge of the carbides during the extraction of the juice to cracking and/or removal from the austenite/ferrite matrix. This behaviour is clearly seen in Fig. 7, where the austenite/ferrite matrix is preferentially removed, leaving narrow channels around the  $M_7C_3$  carbide phases. This would further reduce the efficacy of the weld droplets as the matrix loses its capacity to support the carbides, thus preventing the carbides to withstand greater loads that would improve the gripping and extraction of the cane juice.

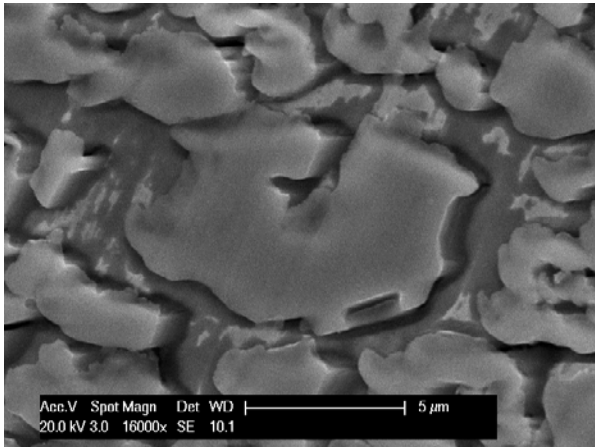


Fig. 7 SEM image of weld droplet (130 A) following 50 hours of immersion in cane juice (sucrose) at 29 °C

### 3. CONCLUSION

Arcing of sugarcane mill roller shells is a common practice done in sugar factories as a way of increasing the efficiency of juice extraction. However, deposited globules generally fail quickly from a variety of surface failures, which include porosity and corrosion.

The microstructure of the weld droplets is clearly hypereutectic, consisting of  $M_7C_3$  carbide phase in an austenite/ferrite matrix, irrespective of the welding current. The results also indicated that arcing done at 130 A with the Elarc Mill Arc 80 electrode optimized the porosity, corrosion and microhardness of the weld droplets, the nominal optimized hardness value being 795 HV.

Corrosion is impacted by the complex interaction of the microstructure, in particular the effect of welding current and porosity. Corrosion was found to have a direct relationship with porosity, and both corrosion and porosity can be minimized by judicious selection of welding current. Within the current range of this study, the optimum corrosion rate and porosity was found to be 1.16 mm/year and 6.6%, respectively, when the arc current was set at 130 A.

### REFERENCES

[1] V.E. Buchanan, P.H. Shipway and D.G. McCartney, "Microstructure and abrasive wear behaviour of shielded metal arc welding hardfacings used in the sugarcane industry," *Wear*, vol. 263, 2007, pp. 99-110.

[2] H. Blaze and D. Gollschewski, "The evolution and development of hardfacing strategies for sugar mill rollers," *Aust. Weld. J.*, vol. 42, 1997, pp. 10-12.

[3] W.S. Coates, "Spotting mill rollers," *Proc. Qld. Soc. Sugar Cane Technol.*, vol. 14, 1947, pp. 81-85.

[4] L.R. George and J.M. Reid, "The sugar mill roller," *Proc. Qld. Soc. Sugar Cane Technol.*, vol. 18, 1951, pp. 75-83.

[5] J.G. Loughran and I. Henderson, "A prototype automated roll arcing machine," *Proc. Aust. Soc. Sugar Cane Technol.*, vol. 14, 1992, pp. 246-252.

[6] D.S. Shann, "Some practical confirmation of experimental milling results," *Proc. Congr. Int. Soc. Sugar Cane Technol.*, vol. 11, 1962, pp. 1040-1046.

[7] G.D. Oliver, "A Tribological Study of Arced Sugar Cane Mill Rolls in Jamaica," Brunel University, PhD Thesis, June 2003.

[8] I.E. French, "The adhesion of chromium carbide-iron weld metal droplets on to sugar mill roller materials," *Met. Forum*, vol. 3, 1980, pp. 55-6.

[9] I.E. French, and D. Klanjscek, "Development of new flux-cored electrodes for arcing of sugar mill rollers," *Proc. Natl. Conf. Aust. Weld. Inst.*, vol. 27, 1979, pp. 29-37.

[10] V.E. Buchanan, "Solidification and microstructural characterisation of iron-chromium based hardfaced coatings deposited by SMAW and electric arc spraying," *Surf. Coat. Technol.*, vol. 203, 2009, pp. 3638-3646.

[11] O.N. Dogan, J. A. Hawk and G Laird II, "Solidification structure and abrasion resistance of high chromium white irons," *Metall. Mater. Trans. A*, vol. 28, 1997, pp. 1315-1328.

[12] G.L.F. Powell, "The microstructure of hypereutectic Cr-C hard surfacing deposits and its dependence on welding variables," *Aust. Weld. Res.*, vol. 6, 1979, pp. 16-23.

[13] T. Ellis and G.G. Garrett, "Influence of process variables in flux cored arc welding of hardfacing deposits," *Surf. Eng.*, vol. 2, 1986, pp. 55-66.

[14] D.E. Crawmer, "Coating structures, properties and materials," in J.R. Davis, Ed., *Handbook of Thermal Technology*, ASM International, 2005.

[15] J.F. Quaas, "Hardfacing international," *Weld. J.*, vol. 49, 1970, pp.75-182.

[16] J.R. Davis, Ed., "Corrosion – Understanding the Basics," ASM International, Materials Park, Ohio, 2000.